HHS Public Access

Author manuscript

Cell Rep. Author manuscript; available in PMC 2020 October 26.

Published in final edited form as:

Cell Rep. 2020 June 09; 31(10): 107754. doi:10.1016/j.celrep.2020.107754.

Rrp6 Moonlights in an RNA Exosome-Independent Manner to Promote Cell Survival and Gene Expression during Stress

Charles Wang[1], **Yanru Liu**[1], **Samuel M. DeMario**[1], **Igor Mandric**[2], **Carlos Gonzalez-Figueroa**[1], **Guillaume F. Chanfreau**[1,3,4,*]

[1]Department of Chemistry and Biochemistry, University of California, Los Angeles, Los Angeles, CA 90095, USA

[2]Department of Computer Science, University of California, Los Angeles, Los Angeles, CA 90095, USA

[3]Molecular Biology Institute, University of California, Los Angeles, Los Angeles, CA 90095, USA

[4]Lead Contact

SUMMARY

The nuclear RNA exosome is essential for RNA processing and degradation. Here, we show that the exosome nuclear-specific subunit Rrp6p promotes cell survival during heat stress through the cell wall integrity (CWI) pathway, independently of its catalytic activity or association with the core exosome. Rrp6p exhibits negative genetic interactions with the Slt2/Mpk1p or Paf1p elongation factors required for expression of CWI genes during stress. Overexpression of Rrp6p or of its catalytically inactive or exosome-independent mutants can partially rescue the growth defect of the *mpk1Δ* mutant and stimulates expression of the Mpk1 p target gene *FKS2*. The *rrp6Δ* and *mpk1Δ* mutants show similarities in deficient expression of CWI genes during heat shock, and overexpression of the CWI gene *HSP150* can rescue the stress-induced lethality of the *mpk1Δrp6Δ* mutant. These results demonstrate that Rrp6p moonlights independently from the exosome to ensure proper expression of CWI genes and to promote cell survival during stress.

In Brief

Wang et al. show that Rrp6 functions with the Slt2/Mpk1 and Paf1 elongation factors for the proper expression of CWI genes during heat stress. The role of Rrp6p in promoting heat-stress-induced gene expression does not require Rrp6 catalytic activity or interaction with the nuclear RNA exosome.

*Correspondence: guillom@chem.ucla.edu.

AUTHOR CONTRIBUTIONS

Conceptualization and Methodology, G.F.C. and C.W.; Investigation, C.W., C.G.-F., and Y.L.; Bioinformatics, S.M.D. and I.M.; Writing—Original Draft, C.W.; Writing—Review and Editing, G.F.C.; Funding Acquisition, G.F.C.

DECLARATION OF INTERESTS

The authors declare no competing interests.

SUPPLEMENTAL INFORMATION

Supplemental Information can be found online at https://doi.org/10.1016/j.celrep.2020.107754.

Graphical Abstract

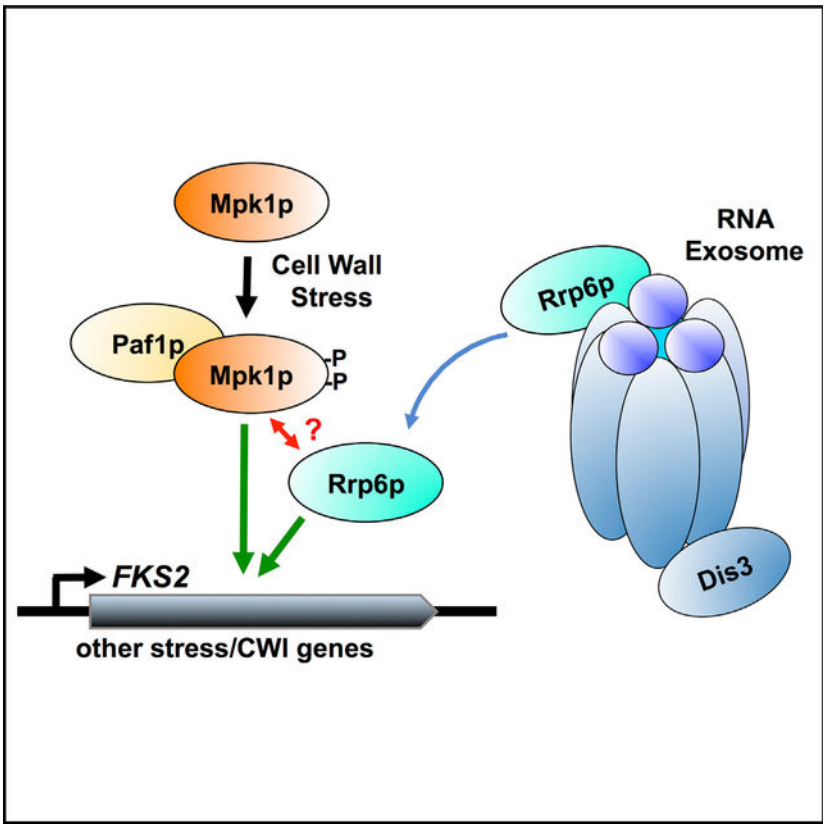

INTRODUCTION

The nuclear RNA exosome complex (which we refer to hereinafter as the nuclear exosome) plays a diverse role in RNA metabolism, from RNA processing to the surveillance and degradation of defective RNAs (Zinder and Lima, 2017). The nuclear exosome is essential for the proper 3'-end trimming and maturation of RNAs including small nuclear RNAs (snRNAs), small nucleolar RNAs (snoRNAs), and ribosomal RNAs (rRNAs) (Allmang et al., 1999; Bernstein and Toth, 2012). Surveillance and degradation of improperly processed RNAs by the exosome limits the export and translation of faulty RNAs that may otherwise be detrimental (Moraes, 2010). Nuclear exosome function is also coupled to regulatory pathways for the proper control of gene expression (Bresson et al., 2017; Volanakis et al., 2013). Mutations within genes encoding exosome subunits are responsible for several human diseases, underscoring the importance of functional RNA exosome activity for cellular homeostasis and proper human development (Fasken et al., 2017; Gillespie et al., 2017; Morton et al., 2018; Wan et al., 2012).

In *S. cerevisiae*, the core ring of the nuclear exosome consists of a family of 6 RNase PH homologs and 3 RNA binding proteins (Bernstein and Toth, 2012; Sloan et al., 2012; Zinder and Lima, 2017). This core contains no exonuclease activity and, instead, relies on two associated proteins for its degradative functions: Dis3p/Rrp44p, which is a processive

exoribonuclease with additional endonuclease activity, and Rrp6p, which has distributive exonucleolytic activity (Bernstein and Toth, 2012; Sloan et al., 2012). *S. cerevisiae* cells lacking Rrp6p are viable, and deletion of the *RRP6* gene has been broadly used as a method to partially inactivate the nuclear exosome. The deletion of *RRP6* results in a slow growth phenotype with an accumulation of many degradation intermediates and unprocessed or 3'-extended RNAs (Burkardand Butler, 2000; Butler and Mitchell, 2010; Feigenbutz et al., 2013a; Fox and Mosley, 2016). Although Rrp6p works within the core exosome to process or degrade its RNA substrates (Wasmuth and Lima, 2017), several studies have suggested an exosome-independent function of Rrp6p (Callahan and Butler, 2008; Fox et al., 2015; Graham et al., 2009).

During stress, specific transcription factors are activated to rapidly alter gene expression and promote cell survival. The mitogen-activated protein kinase (MAPK) cascade is an evolutionary conserved pathway that regulates these transcription factors during environmental stress (Gustin et al., 1998; Hahn and Thiele, 2002; Kim et al., 2010; Levin, 2005). Mpk1p/Slt2p is a kinase involved in the cell wall integrity (CWI) pathway, a MAPK cascade that monitors and maintains the integrity of the cell wall in *S. cerevisiae* (Figure 1A; Kim and Levin, 2011). Once activated by upstream kinases, Mpk1p performs multiple functions to alter gene expression; it phosphorylates the transcription factors Rlm1p and Swi4p/Swi6p to stimulate their binding to DNA (Figure 1A), regulates transcription initiation and elongation directly through a non-catalytic mechanism involving the Paf1 complex (Figure 1A), and retains the bulk of mRNAs within the nucleus through an unknown mechanism (Carmody et al., 2010; Jin et al., 2014; Kim et al., 2010). In addition, Mpk1p directly influences RNA polymerase II (RNAPII) activity by phosphorylating the Tyr1 residues of the YSPTSPS repeats of the C-terminal domain (CTD) of its large subunit (Yurko et al., 2017). Altogether, these molecular responses result in a remodeling of the cell wall composition and an overall increase in the thermotolerance of the cell (de Nobel et al., 2000). Perturbation of the activity of CWI factors results in the downregulation of a subset of cell wall proteins and, consequently, a decrease in the ability of cells to handle their internal turgor pressure (de Nobel et al., 2000; Levin, 2005). This results in a osmoremedial lethal phenotype at high temperatures (de Nobel et al., 2000; Levin, 2005).

In this study, we provide genetic evidence for a role for Rrp6p in promoting cell survival during heat stress through the CWI pathway, and we show that Rrp6p contributes to proper gene expression during stress in a manner similar to that of Mpk1p. The role that Rrp6p plays in this pathway is independent of its RNase activity and of its association with the nuclear exosome. These data identify an exosome-independent function for Rrp6p in synergizing the roles of the Mpk1p and Paf1p elongation factors in the proper induction of the CWI gene expression program during stress.

RESULTS

Rrp6p Plays a Critical Role in the Heat Stress Response Pathway of *S. cerevisiae*

S. cerevisiae strains lacking Rrp6p are viable, but loss of Rrp6p results in a temperature-sensitive (ts) phenotype (Figure 1B). Although this phenotype could be due to a destabilization of the core exosome at higher temperatures in the absence of Rrp6p, it could

also indicate that Rrp6p plays an exosome-independent role during cellular stress. To investigate this potential role, we deleted Rrp6p in conjunction with the MAPK Slt2p, also known as Mpk1p. The absence of Mpk1p compromises the CWI pathway and sensitizes yeast cells to specific cell wall stresses, including growth at higher temperatures (de Nobel et al., 2000). Strikingly, the *mpk1Δrrp6Δ* double mutant was not viable at 37°C, a phenotype much more severe than the slow growth of the single mutants at the same temperature (Figure 1B). As growth at 37°C induces cell wall stress, we hypothesized that this synthetic lethality might be due to a weakened cell wall with an inability to tolerate differences in osmotic potential. If so, addition of osmotic support should restore the growth of the double mutant. As predicted, the lethality of the *mpk1Δrrp6Δ* strain at 37°C was rescued by the addition of 1 M sorbitol or 0.6 M KCI (Figure 1C). This result indicates that lethality of the *mpk1Δrrp6Δ* strain at 37°C is a direct result of compromised cell wall integrity, potentially because of improper expression of cell wall proteins. Osmotic support had no additional effect on the growth of the *rrp6Δ* single mutant, suggesting that the potential role for Rrp6p in the CWI pathway is not the growth-limiting factor for this single mutant at 37°C.

We next asked whether the lethality of the *mpk1Δrrp6Δ* strain at higher temperatures was specific to the absence of the nuclear exonuclease Rrp6p or whether the inactivation of cytoplasmic RNA processing or degradation factors may exhibit similar phenotypes. To answer this question, we deleted Mpk1p along with the cytoplasmic exoribonuclease Xrn1p, the nonsense-mediated decay factor Upf1p, or the cytoplasmic RNA exosome factor Ski2p (Parker, 2012). These mutants were chosen to disable a variety of RNA processing and degradation processes. However, none of these double mutations phenocopied the synthetic lethality of *mpk1Δrrp6Δ* cells (Figure S1A). This result shows that the lethality of the *mpk1Δrrp6Δ* mutant is specific to the absence of Rrp6p. Altogether, these data demonstrate a specific negative genetic interaction between Rrp6p and Mpk1p, suggesting that the two proteins may cooperate to maintain the integrity of the cell wall and promote cell survival under heat stress.

The Role of Rrp6p in the Heat Stress Response Pathway Is Independent of Its Catalytic Activity or Association with the Core Exosome

The previous observations raised the question of how Rrp6p and Mpk1p cooperate to promote cell survival during growth at non-permissive temperatures. RNA processing or degradation defects associated with the absence of Rrp6p may impede the rapid changes of mRNA abundance and gene expression that are necessary for adaption to environmental stresses. If the temperature sensitivity of the *mpk1Δrrp6Δ* mutant were due to a general deficiency in nuclear exosome function at high temperatures, a similar lethal phenotype would be expected if the *mpk1Δ* mutation were combined with other mutations that inhibit nuclear exosome functions. This can be achieved through the removal of the nuclear exosome cofactors Rrp47p or Mpp6p orthrough a point mutation within the core exosome protein Rrp40 (*rrp40-W195R*) that prevents its stable association with the exosome complex and its nuclear cofactor Mpp6p (Butler and Mitchell, 2010; Fasken et al.,2017; Gillespie et al., 2017). Strikingly, both *mpk1Δrrp47Δ* and *mpk1Δrrp40-W195R* mutant strains were viable when grown at high temperatures and, in fact, grew better than the single *mpk1Δ* mutant alone (Figure 1D). A similar growth rescue was observed in the *mpk1Δmpp6Δ*

mutant at 37°C as well (Figure S1B). These results suggest that the lethality of the *mpk1Δrrp6Δ* strain is not due to a general inactivation of the nuclear exosome but rather because of an exosome-independent function of Rrp6p. The *rrp40-W195R* mutation or the loss of Mpp6p did not impact Rrp6p protein levels compared to wild type (WT) at 37°C (Figure S2A), but a decrease of Rrp6p protein abundance was detected in the *rrp47Δ* mutant at 37°C (Figure S2A), as previously reported (Feigenbutz et al., 2013b). Because Rrp6p protein levels were not affected in a consistent manner, we postulate that the fitness gain detected in these double mutants at elevated temperatures compared to the *mpk1Δ* mutant could be due to a relative increase in the free pool of Rrp6p arising from the destabilizing effect of the absence of Rrp47p, Mpp6p, orthe Rrp40p mutations on Rrp6p association with the exosome. To further test this hypothesis, we deleted the chromatin remodeler Isw1p, which cooperates with Rrp6p to promote mRNA retention during stress (Babour et al., 2016). Indeed, Isw1p deletion also rescued the heat sensitivity of the *mpk1Δ* mutant (Figure 1D), consistent with the idea that dissociating Rrp6p from any of its associated factors (Isw1p or the nuclear exosome) can positively impact the CWI response. Finally, overexpression of Rrp6p independently from any other exosome component improved the growth of the *mpk1Δ* mutant at 37°C (Figures 1E and 2D). This result demonstrates that other core exosome subunits are not required to mediate the role that Rrp6p plays in promoting cell survival during stress.

To further explore the hypothesis of an exosome-independent function of Rrp6p in the stress response pathway, we expressed a mutant form of Rrp6p, *rrp6-C2Δ* (Figure 2A), that cannot associate with the nuclear exosome (Callahan and Butler, 2008) and tested its ability to promote the growth of the *mpk1Δ* mutant at 37°C. Strikingly, overexpression of *rrp6-C2Δ* improved the growth of the *mpk1Δ* mutant under heat stress (Figure 2D). We next determined whether the expression of *rrp6-C2Δ* may rescue the growth lethality of the *mpk1Δrrp6Δ* mutant at high temperatures. Because strains were grown on minimal media for plasmid selection, the lethality of the *mpk1Δrrp6Δ* strain was detected at a lower temperature (35°C). Remarkably, expression of the *rrp6-C2Δ* mutant rescued the growth of the *mpk1Δrrp6Δ* mutant at 35°C and promoted a growth rate similar to that of the *mpk1Δ* mutant harboring an empty vector (Figure 2B). This effect was not due to differences in protein stability, as no detectable differences in protein abundance were observed between the exogenously expressed WT Rrp6p and the C2Δ mutant before and after heat stress (Figure S2B). These results provide further support to the conclusion that Rrp6p plays a role in the CWI pathway independently from its involvement with the nuclear exosome.

A role for Rrp6p in promoting cellular survival independently from the nuclear exosome may or may not require its exonuclease catalytic activity. We expressed a catalytically inactive version of Rrp6p void of all exonuclease activity (*rrp6-D238N*; Callahan and Butler, 2008; Figure 2A) to determine whether Rrp6p catalytic activity is necessary to improve the growth of the *mpk1Δ* mutant at 37°C. This *rrp6-D238N* mutant did not improve the slow growth phenotype of the *rrp6°* mutant under heat stress when expressed exogenously (Figure 2C). Nonetheless, expression of the *rrp6-D238N* mutant improved the growth of the *mpk1Δ* mutant at 37°C (Figure 2D). In fact, expression of either the *rrp6-D238N* or the *rrp6-C2Δ* mutant rescued the growth of the *mpk1Δ* mutant more so than the expression of WT *RRP6* (Figure 2D). While the *rrp6-D238N* mutant was expressed at levels slightly higher than that

of WT Rrp6p in stress conditions (Figure S2B), the fact that the *rrp6-C2Δ* mutant was expressed at levels comparable to that of WT before and after heat stress (Figure S2B) shows that the ability of these two *rrp6* mutants to rescue the growth of the *mpk1Δ* mutant better than WT Rrp6p is not due to increased Rrp6p levels. These data suggest that these mutants may be better catered to fulfilling Rrp6p's stress response functions without the restraint of its exosome or exonuclease functions. In addition, the catalytically inactive Rrp6p mutant rescued the growth of the *mpk1Δrrp6Δ* strain at a high temperature, showing that the function of Rrp6p in the stress response pathway is, indeed, independent of its exonuclease activity (Figure 2C). To ascertain the absence of any exonuclease activity that may contribute to the rescue of growth, northern blot analysis was performed with probes corresponding to the ITS2 region of the rRNA, a *bona fide* substrate of the nuclear exosome (Callahan and Butler, 2008). As expected, an increase in the 7S rRNA processing intermediate was detected in the *rrp6Δ* and *mpk1Δrrp6Δ* mutants carrying an empty vector, as these mutants lack Rrp6p to efficiently process this intermediate (Figure S2E, lanes 5 and 7). Similarly, an accumulation of the 7S was detected when the catalytically inactive Rrp6p mutant was expressed in the *rrp6Δ* and *mpk1Δrrp6Δ* mutant strains, confirming that *rrp6-D238N* is, indeed, catalytically inactive (Figure S2E, lanes 6 and 8). Moreover, expressing the *rrp6-D238N* mutant negatively impacted rRNA processing in strains lacking the endogenous WT Rrp6p, as shown by a higher accumulation of the 7S rRNA intermediate in these strains (Figure S2E, lanes 6 and 8) compared to the *rrp6Δ* and *mpk1Δrrp6Δ* mutants alone (Figure S2E, lanes 5 and 7). We speculate that the catalytically inactive *rrp6-D238N* mutant may further inhibit 7S processing by binding to and stabilizing this rRNA intermediate and preventing further trimming by the core exosome. Thus, despite exacerbating rRNA processing defects, a catalytically inactive *rrp6-D238N* mutant can still promote survival of the *mpk1Δrrp6Δ* strain in stress conditions, further strengthening the idea that Rrp6p functions independently from the RNA exosome during stress.

To further explore the protein domains of Rrp6p involved in its stress-related functions along Mpk1p, we used a C-terminally TAP-tagged version (Figure 2A), which we originally thought of using for proteomics studies. Strikingly, the Rrp6p-TAP strain was unviable at 37°C (Figure 2E). This phenotype is not due to thermal instability of the TAP-tagged version of Rrp6p, as it is expressed similarly to WT at all temperatures (Figure S2C). Despite normal expression, the TAP-tagged version of Rrp6p is clearly defective for exosome function, as shown by an accumulation of 7S similar to that of the *rrp6Δ* strain at all temperatures (Figure S2F). This result could be due to the role of the C terminus of Rrp6p in promoting exosome activity (Wasmuth and Lima, 2017), which may be compromised by the addition of a TAP tag at the C terminus. However, unlike the *rrp6Δ* strain, the growth phenotype of the Rrp6-TAP strain at elevated temperatures could be rescued by adding sorbitol (Figure 2E), showing that the lethality of the TAP-tagged strain at 37°C is not due to inactivation of the exosome but rather to the inability of the TAP-tagged version of Rrp6p to function in the CWI pathway. Altogether, these data demonstrate that delayed or defective RNA processing is not responsible for the lethality of the *mpk1-Δrrp6Δ* mutant at high temperatures and that the involvement of Rrp6p in the stress response is independent of its exonuclease activity or association with the nuclear exosome.

Rrp6p Function in the CWI Pathway Requires the Interaction between Mpk1p and Paf1p

We next sought to genetically explore the role that Rrp6p plays in the CWI pathway. To this end, we generated mutants in which Rrp6p is deleted along with several CWI factors depicted in Figure 1A. These included the pseudokinase Kdxlp; the downstream transcription factor Swi4p; and the RNAPII-associated elongation factor Paf1p, which functions downstream of Mpk1p (Levin, 2005). The *kdx1Δrrp6Δ*, *swi4Δrrp6Δ*, and *paf1Δrrp6Δ* mutant strains were monitored for growth at 30°C or 37°C. There was no detectable growth defect associated with the *swi4Δrrp6Δ* or *kdx1Δrrp6Δ* mutants at 37°C (Figure S3A). However, similarly to the *mpk1Δrrp6Δ* mutant, the *paf1Δrrp6Δ* mutant was not viable at high temperatures (Figure 3A), strengthening the connection between Rrp6p and the branch of the CWI pathway regulated by Mpk1p and Paf1p (Figure 1A).

Further experiments showed that the phenotype of the *paf1Δrrp6Δ* mutant mirrors that of the *mpk1Δrrp6Δ* mutant. The lethality of the *paf1Δrrp6Δ* mutant at a high temperature could be rescued through the addition of osmotic support (Figure 3A), or by expressing *rrp6-C2Δ* (Figure S3B), but not the *rrp6-D238N* mutant. As Paf1p is involved in many aspects of transcription (Van Oss et al., 2017), its absence may attenuate multiple processes in addition to CWI, which could explain the inability of the *rrp6-D238N* mutant to rescue the growth lethality of the *paf1Δrrp6Δ* mutant at 35°C. Nonetheless, these results indicate that the role of Rrp6p in the CWI pathway involves Mpk1p and the downstream RNA-polymerase-associated factor Paf1p. As Paf1p resides within the Paf1 complex (Paf1C), we tested whether co-deletion of Rrp6p and other Paf1C-associated factors such as Leo1p and Rtf1p would exhibit a similar growth defect under heat stress. The absence of both Rtf1p and Rrp6p did not have any major impact on growth at 30°C and at 37°C (Figure 3B). However, co-deletion of Rrp6p and Leo1p resulted in a severe slow growth phenotype compared to the single mutants alone (Figure 3B). This result confirms the genetic interaction between Rrp6p and the Paf1 complex and suggests a possible molecular basis for the lethality of *mpk1Δrrp6Δ* at 37°C. The absence of Leo1p may not impact the function of the Paf1c to the same extent as deleting Paf1p, which may explain why the *leo1Δrrp6Δ* mutant was not lethal at 37°C. This is consistent with the observation that only the single *paf1Δ* mutant displays a slow growth phenotype when compared to *leo1Δ* and *rtf1Δ* alone (Figure 3B) and with previous studies showing that Paf1p is critical for the stability of the Paf1 complex (Van Oss et al., 2017).

We next asked whether the role of Rrp6p in the CWI pathway requires the interaction of Mpk1p with Paf1p and/or its kinase activity. To this end, we used strains expressing either a version of Mpk1p void of its kinase activity (*mpk1-K54R*) or a nonphosphorylatable mutant form (*mpk1-TAYF*). The *mpk1-TAYF* mutant cannot be phosphorylated by upstream factors, which prevents it from associating with Paf1p (Kim and Levin, 2011). By contrast, the catalytically inactive *mpk1-K54R* mutant can interact with Paf1p but is incapable of phosphorylating other downstream factors. Strikingly, the expression of the *mpk1-TAYF* mutant did not rescue the growth of the *mpk1Δrrp6Δ* strain at 35°C (only suppressor colonies were observed), while the *mpk1-K54R* mutant rescued the growth of the *mpk1Δrrp6Δ* mutant under heat stress (Figure 3C). The differences in growth rates between the different versions of Mpk1p were not due to differences in protein stability, as the two

mutant versions were expressed to levels similar to or slightly lower than those of WT Mpk1p (Figure S2D). Overall, these results show that Rrp6p is involved in promoting heat stress response in a specific branch of the CWI pathway (Figure 1A) that requires the ability of Mpk1p to interact with the downstream factor Paf1p to regulate gene expression, but it does not require its kinase activity.

Rrp6p Promotes Proper CWI Gene Expression during Heat Stress Independently of the Nuclear Exosome or of Its Catalytic Activity

Mpk1p and Kdx1p promote transcriptional elongation of stress-responsive CWI genes, such as *FKS2*, through a physical interaction with Paf1p (Kim and Levin, 2011), and the absence of Mpk1p and Kdx1p results in a slow growth phenotype at 37°C (Figure S3A). To determine whether Rrp6p may play a role in CWI gene expression, we overexpressed Rrp6p in WT and *mpk1Δkdx1Δ* strains and analyzed *FKS2* expression during heat shock. Strikingly, Rrp6p overexpression increased *FKS2* levels in both strains (Figure 4A). By contrast, the overexpression of Rrp6p did not increase the transcript abundance of *RPS12*, which is repressed before and after heat shock in the *mpk1Δkdx1Δ* mutant (Figure 4B). This suggests that the overexpression of Rrp6p does not stabilize RNA transcripts on a global scale through altering exosome activity but specifically promotes expression of stress-induced genes. The overexpression of *rrp6-C2Δ* in the *mpk1Δkdx1Δ* mutant also significantly increased *FKS2* transcript levels post-heat shock (Figure 4C). Overexpression of the *rrp6-D238N* mutant showed a non-statistically significant increase, possibly due to the pleiotropic effects of this mutant that contributed to an increased variability between replicates. Nonetheless, these RNA analyses corroborate our previous observation that the overexpression of *RRP6* can enhance the growth of the *mpk1Δ* mutant at 37°C (Figure 2D) and identify a role for Rrp6p in the expression of CWI target genes. These results also suggested that the lethality of the *mpk1Δrrp6Δ* strain at 37°C is due to changes in gene expression that result in a defective cell wall and led us to perform RNA-sequencing (RNA-seq) analysis of the *mpk1Δrrp6Δ* mutant and of control single-mutant and WT strains before and after a 45-min heat shock at 42°C. Although this heat shock condition is different from the temperatures used previously for growth at steady state, it was chosen to detect rapid responses to heat stress at the RNA level without attenuation due to longer exposures.

RNA-seq analysis revealed the repression of a large number of genes in the *mpk1Δ*, *rrp6Δ*, and *mpk1Δrrp6Δ* mutant strains compared to WT in heat shock conditions (Figure 4D). By contrast, the number of genes downregulated compared to the WT before heat shock was much lower in all of these mutants (Figure 4D, left). Most notably, the large majority of genes repressed in heat shock compared to the WT is shared between the *mpk1Δ* and *rrp6Δ* mutant strains (Figure 4D), which further support a shared biological function between these two proteins during stress. Importantly, this overlap is much less pronounced for RNAs repressed in these mutants prior to heat shock, further supporting a similar role for Rrp6p and Mpk1p during heat shock. The full list of genes up- or downregulated in each of the mutants is presented in Table S1. Gene Ontology (GO) analysis of repressed genes shared between the *mpk1Δ* and *rrp6Δ* mutant strains in heat shock conditions showed an enrichment for cell wall proteins, protein transporters, and ribosomal protein genes (RPGs) (Table S1). However, we do not think that the decrease in RPG expression is due to a direct

role for Rrp6p in their expression, as Rrp6p overexpression could not rescue the downregulation of *RPS12* detected in the *mpk1Δkdx1Δ* mutant (Figure 4B). Analysis of cell wall gene expression revealed a large decrease in the expression of *HSP150* in the *mpk1Δrrp6Δ* mutant under heat shock. This decrease in *HSP150* expression may play a significant role in the phenotype of the double mutant, as *HSP150* encodes a cell wall protein necessary for cell wall stability (Russo et al., 1992). Although we were unable to detect an increase in *HSP150* expression in our heat shock conditions, the decreased expression in the *mpk1Δrrp6Δ* mutant was confirmed by northern blot analysis (Figure 5A). The decrease in *HSP150* expression was not due to a general defect in the expression of heat shock protein genes, as *HSP12* was still robustly induced in the *mpk1Δrrp6Δ* mutant (Figure 5A). The overexpression of Rrp6p and its mutant forms had no significant effect on *HSP150* expression in the *mpk1ΔkdxΔ* mutant during heat shock (Figure S4A), suggesting that robust expression of *HSP150* requires both Rrp6p and Mpk1p.

HSP150 Overexpression Promotes Survival of the *mpk1Δrrp6Δ* Mutant in Heat Stress

Based on the previous observations, we hypothesized that a defect in *HSP150* expression may be a contributing factor in the inability of the *mpk1Δrrp6Δ* strain to survive under heat stress. To test this hypothesis, we constructed an *HSP150* overexpression system using the multicopy vector YEp24 (Parent et al., 1985) and a *TEF1* promoter. The use of this promoter alleviates any potential decrease in *HSP150* expression that might be dependent on its endogenous promoter and its association with stress-specific transcription factors. Strikingly, *HSP150* overexpression promoted survival of the *mpk1Δrrp6Δ* mutant under heat stress (Figure 5B). Importantly, the overexpression of *HSP150* did not rescue the growth of another severely heat-sensitive mutant strain lacking the RNase III endonuclease Rnt1p (Roy and Chanfreau, 2014) at the same temperature (Figure 5C). This result shows that the *HSP150* overexpression rescue effect is specific to *mpk1Δrrp6Δ* cells and does not promote growth rescue of all ts strains. We note that *HSP150* overexpression does not fully rescue the growth of the *mpk1Δrrp6Δ* mutant, as it is highly likely that other improperly expressed genes may also contribute to the lethality of the *mpk1Δrrp6Δ* mutant strain at elevated temperatures, despite *HSP150* being a major contributor. Taken together, these results show that Rrp6p along with Mpk1p and, possibly, Paf1p are required to ensure proper expression of *HSP150* and other CWI genes, which promote cell survival during stress.

How Mpk1p, Paf1p, and Rrp6p cooperate to ensure proper gene expression during heat stress remains unknown. We were unable to detect a stable interaction between Rrp6p and Mpk1p based on co-immunoprecipitation experiments (Figure S5A). Since the role of Rrp6p in stress is independent from its exonuclease activity, we hypothesized that the stress-induced expression of RNAs stemming from the CWI pathway requires Rrp6p for proper transcription. This led us to investigate whether Rrp6p may alter RNAPII phosphorylation state. Mpk1p has been shown to phosphorylate the Tyr1 residues of the C-terminal domain (CTD) of RNAPII during multiple stress responses and impact gene expression (Yurko et al., 2017). However, no differences in Pol.II CTD Tyr1 phosphorylation were observed in our mutant strains under heat stress (Figure S5B). Further studies are required to precisely identify the role Rrp6p plays with Mpk1p and Paf1p to promote cell survival during stress.

DISCUSSION

In this study, we demonstrate an undiscovered yet critical role of Rrp6p in promoting cellular survival during heat stress. This role is remarkably independent of both its catalytic activity and its association with the nuclear exosome. This unique function of Rrp6p includes, but may not be limited to, its ability to synergize the roles of the Mpk1p and Paf1p to promote proper expression of CWI genes to ensure CWI. Although further biochemical work is necessary to characterize the precise mechanism behind this unique function of Rrp6p, our results show that it may be linked to the necessity of expressing specific mRNAs during stress. Strikingly, restoring the expression of a single target gene, *HSP150*, was sufficient to rescue the growth of the *mpk1Δrrp6Δ* mutant at high temperatures. This result and the osmoremedial phenotype of this mutant provide major evidence for the fact that defective induction of CWI genes caused by simultaneous inactivation of Mpk1 and Rrp6p is the direct cause of cellular lethality. However, it is likely that defective expression of a diverse subset of genes in the absence of Rrp6p may partially contribute to the overall decrease of cellular fitness in this background as well.

Interestingly, the RNA exosome has been linked previously to stress-related gene expression, as work in *Drosophila* has shown that the exosome associates with heat shock genes (Andrulis et al., 2002). However, the data presented here suggest that the role of Rrp6p during stress in yeast is independent of the core exosome, as demonstrated by the results obtained with mutants that impact other exosome subunits or by overexpressing Rrp6p and its exosome-independent C2Δ mutants, all of which have a positive effect on cell survival through the CWI pathway (Figures 1D, 1E, and 2B—2D). This suggests that the mechanisms involving the exosome in stress-related gene expression may have diverged during evolution. Rrp6p has also been shown to function along Isw1p in mRNP retention at the site of transcription during heat shock (Babour et al., 2016). However, we found that the genetic inactivation of Rrp6p and Isw1p have opposite effects when combined with Mpk1p inactivation (Figure 1D), which shows that the role of Rrp6p in the CWI pathway is not linked to its function in mRNP retention during stress.

The concept of an exosome-independent role of Rrp6p in the CWI pathway implies that Rrp6p must exist in the cell as a free pool during stress, perhaps as a result of increased synthesis, or by dissociating from the core exosome. We did not detect an increase of Rrp6p expression during heat shock (Figures S2B, S2C, and S5A), which seems to eliminate the former hypothesis. Thus, it is possible that a subpopulation of Rrp6p may dissociate from the core exosome during stress so that Rrp6p may fulfill its function in the CWI pathway. Alternatively, it is possible that Rrp6p newly synthesized after heat shock may not associate with the core exosome but, instead, function independently and possibly associate with the chromatin to promote proper transcriptional elongation along with Mpk1p and Paf1p. Such association with the chromatin to modulate transcriptional complexes would not be unexpected, as Rrp6p has been shown to mediate transcriptional termination (Fox et al., 2015).

Altogether, this study demonstrates a specialized function of Rrp6p in promoting gene expression independently of the RNA exosome core and of its ribonucleolytic activity.

Although this function operates in the context of the CWI pathway, it is possible that Rrp6p may also function in other biological processes under various cellular growth conditions. The full extent of Rrp6p influence on RNA metabolism remains to be explored and may provide further evidence on the substantial functional complexity of this protein in cellular physiology.

STAR * METHODS

RESOURCE AVAILABILITY

Lead Contact—Requests for information, resources, and materials will be fulfilled by the lead contact, Guillaume Chanfreau (guillom@chem.ucla. edu), without restrictions.

Materials Availability—All unique reagents generated in this study (Yeast strains and plasmids) are available from the Lead Contact without restriction. For further information and requests, please contact Guillaume Chanfreau.

Data and Code Availability—RNA Sequencing datasets generated in this study are deposited under the accession GEO: GSE140504.

EXPERIMENTAL MODEL AND SUBJECT DETAILS

Strains construction—Unless otherwise noted, all strains used in this study were either obtained from the GE Dharmacon Yeast Knockout collection or derived from BY4742 and listed in Supplemental Material (Table S2). Mutant strains were constructed using the lithium acetate/ PEG/Single stranded carrier DNA transformation method (Gietz and Schiestl, 2007) with PCR products containing flanking regions of the area of interest for homologous recombination. The PCR products used in these transformations were produced from template plasmids as described in Longtine et al. (1998). Transformants are grown on plates supplemented with antibiotics and/or on drop out plates before being streaked for single colonies. Successful transformants are confirmed through the extraction of its genomic DNA to be used for PCR using primers specific to the region of interest. Incorporation of plasmids into yeast was performed using the same lithium acetate/PEG/ Single stranded carrier DNA transformation method mentioned above.

Yeast culturing—Yeast cultures were grown in either YPD (1% w/v yeast extract, 2% w/v peptone, and 2% w/v dextrose) or in appropriate drop out minimal media (0.67% w/v yeast nitrogen base, 2% w/v dextrose, and 0.2% w/v amino acid mixture). Unless otherwise described, 50ml cultures were grown at the standard 30°C to exponential phase (OD_{600nm} of ~0.4–0.6) for spot dilution analysis or to be flash frozen in liquid nitrogen for downstream usage. For heat shock experiments, cells were grown at 23°C steady state to an OD_{600nm} of ~0.4–0.6 before equal volumes of prewarmed media was added to acquire the desired final temperature.

Cloning and bacterial transformations—All PCRs done for cloning uses the high-fidelity polymerase Phusion Hi-Fi (New England Biolabs). Cloning of *RRP6* into YEp24 was done using standard procedures. Briefly, the *RRP6* template was PCR amplified with

primers flanked by Sac1 or Sphl restriction cut sites. The template was then cut by the respective restriction enzymes before being column purified (Biopioneer). The YEp24 vector was cut by the same restriction enzymes before being treated with CIP phosphatase (New England Biolabs) prior to column purification. Ligation of the insert and vector were done using a T4 DNA ligase (Life Technologies) before being transformed into competent DH5α E.coli cells. Transformed cells were plated on LB plates supplemented with ampicillin and positive clones were confirmed through colony PCR.

Cloning of *HSP150* with a TEF1 promoter in YEp24 was done using a Quick-Fusion cloning kit (Bimake). Here, the *TEF1* promoter was PCR amplified using the pFA6a-FRB-KANMX as a template (Longtine et al., 1998). The amplified *TEF1* promoter product was designed to contain a BamHI cut site in its 5'end and overlapping regions with the *HSP150* template in its 3'end. The *HSP150* template was amplified from yeast genomic DNA. This *HSP150* template was designed to contain a homology region to the *TEF1* promoter template on its 5'end and a Sphl restriction cut site on its 3'end. These PCR products along with a linearized YEp24 vector were used in the Quick-Fusion Cloning reaction according to manufacturer protocol. All oligonucleotides used are found in Table S4

Plasmid site directed mutagenesis—The YEp24 plasmids containing the mutant forms of *RRP6* were created through site-directed mutagenesis using the QuikChange Lightning Site-Directed Mutagnesis Kit (Agilent Technologies) according to manufacturer protocol. The oligonucleotides used were designed by the online QuikChange Primer Design tool and can be found in the Table S4

Yeast spot dilutions—Yeast cultures were grown to an exponential phase of OD_{600nm} of ~0.4–0.6 in appropriate media. Within a 96 well plate, each culture was then diluted to an OD_{600nm} of 0.05 in 100uL of media. Serial dilutions were performed 5 times, where each time a 30uL of cell suspension was added to 100uL of media. 5uL of the final serial dilution were spotted on either YPD or the appropriate drop out plate. The plates are left to dry before incubation at the indicated temperature and for the indicated number of days of growth. Each spot dilutions have been done for a minimum of two replicates.

METHOD DETAILS

Yeast genomic DNA isolation—Approximately 100uL in volume of yeast were collected from a freshly streak patch and placed in a safe-lock Eppendorf tube. The cells were resuspended in 200uL of lysis buffer (10mM Tris-HCl pH 7.4, 1mM EDTA pH 8 and 3% SDS) and incubated at 65°C for 5 min. Afterward, 400uL of TE buffer was added to the samples along with 600uL of phenol-chloroform (phenol: chloroform: isoamyl alcohol 25:24:1, pH 8, Millipore Sigma). The samples were vortexed for 1 min and centrifuged at 15,000 rpm for 5 min. The top aqueous layer was transferred to a new tube containing 1ml of cold 100% isopropanol to encourage the precipitation of DNA. The samples were centrifuged at 15,000 rpm for 10 min and the supernatant was removed. The gDNA pellet was washed once with 200uL of 70% ethanol before being resuspended in 100uL of pure water.

RNA extraction—To the frozen cell pellets, 500 μL of phenol: chloroform: isoamyl alcohol (25:24:1, pH 6.7, Omni Pur), 400 μL of acid-washed beads and 500 μL of RNA buffer (50 mM Tris-HCl pH 7.5, 100 mM NaCl, 10mM EDTA, 2% SDS w/v) were added and vortexed for 1 min. The samples were incubated at 65°C for 6 min before being vortexed for another min. Afterward, the samples were spun down at 13,200 rpm for 5 min before 450 μL of the aqueous layer was transferred to a new Eppendorf tube containing 450 μL of fresh phenol: chloroform: isoamyl alcohol. The mixture was vortexed for an additional min before being spun down at 15,000 rpm for 2 min. About 400 μL of the top aqueous layer was transferred to a new Eppendorf tube containing 1 ml of 100% ethanol and 40 μL of 3M sodium acetate pH 5.2. The samples were then cooled to −80°C for 30 min to facilitate precipitation of the RNA. The samples are then spun down for 10 min at 15,000 rpm to pellet the precipitated RNA. The supernatant was then removed, and the RNA pellet washed with 200 μL of 70% ethanol. The clean RNA pellets were resuspended in 40–80 μL of nuclease-free water before being quantitated using the NanoDrop (Thermoscientific).

Riboprobe synthesis and oligoprobe radiolabeling for northern blot analysis—Radiolabeled riboprobes were transcribed *in vitro* using T3 RNA polymerase (Promega) according to the manufacturer protocol. However, α-^{32}P-UTP (Perkin Elmer) was used in lieu of α-^{32}P-CTP. The template used in the *in vitro* transcription were synthesized through PCR using primers corresponding to the gene of interest (Table S4). After synthesis, the riboprobes are directly transferred into hybridization bottles containing the pre-hybridized membranes.

Radiolabeled oligoprobes were synthesized using a T4 polynucleotide kinase (New England Biolabs) and γ-^{32}P-ATP (Perkin Elmer) according to manufacturer protocol. The oligonucleotides used in this procedure can be found in the Table S4.

Northern blot analysis—5 μg of total RNA were normalized to the same volume among all samples. The RNA aliquots were carefully combined with 4 times its volume of glyoxal buffer [60% DMSO (Sigma-Aldrich), 20% glyoxal v/v (Sigma-Aldrich), 5% glycerol, 40 μg/ml ethidium bromide, 1X BPTE pH 6.5 (10 mM PIPES (Sigma-Aldrich), 30 mM Bis-Tris (Sigma-Aldrich), 10 mM EDTApH 8.0)] and incubated at 55°C for 1 h. The samples are then cooled on ice for an additional 5 min before being loaded onto 1.8% agarose gels made with 1X BPTE buffer. Electrophoresis was performed with 1X BPTE running buffer at 120V for 3–5 h. After sufficient separation, the gel was washed with deionized water for 10 min, 75mM NaOH for 15 min, and in 10X SSPE buffer (100 mM sodium phosphate, 1.5 M NaCl, and 100 mM EDTA, pH 7.4) for 10 min. The RNA was then transferred overnight from the agarose gel to an Amersham Hybond-N$^+$ membrane (GE Healthcare Life Sciences) using 10X SSPE. All membranes are cross-linked with Stratalinker UV Crosslinker 2400 (Stratagene) and if necessary, stored in 2X SSPE buffer at 4°C. The membranes are pre-hybridized in Churchs buffer (1 % BSA w/v, 1 mM EDTA, 0.5M sodium phosphate pH 7.2, 7% SDS v/w) at 65°C for 1 h before radiolabeled riboprobes are added directly into the buffer. The membranes are hybridized overnight before being washed twice with 2X SSPE, 0.1% SDS for 10 min each, and then twice with 0.1 X SSPE, 0.1% SDS for 10 min each as well. For visualization, the washed blots are exposed to K-screens (Kodak) from several h to

up to 2 days depending on the strength of the signal. The screens are then scanned using the Bio-Rad FX Imager. Images were quantified using imageJ, and analyzed and plotted using GraphPad.

Western blot analysis—Flash frozen cell pellets were lysed using a high salt lysis buffer containing 200mM Tris-HCl pH 8.0, 320mM Ammonium Sulfate, 20mM EDTA pH 8.0, 10mM EGTA pH 8.0, 5mM $MgCl_2$, 1mM DTT, 20% glycerol, 1mM PMSF and 1x protease inhibitor cocktail (Roche). Approximately 400uL of acid washed beads (Sigma) were added to the samples before being vortexed at 4°C for 3 min 5 times, with 1-min breaks in between. The samples were briefly spun down and transferred to a new Eppendorf tube, leaving the glass beads behind. Cellular debris was pelleted down through centrifuging the samples at max speed for 10 min in a pre-chilled 4°C centrifuge. Protein concentration was quantitated using a Bradford protein assay (Bio-Rad).

5ug of protein were prepared with 1x SDS loading dye and 3.1 % β-mercaptoethanol before being boiled for 5 min prior to loading on a 10% SDS-Page gel. After sufficient separation, the samples were transferred onto a PVDF membrane and blocked in 5% milk in PBS-T overnight at 4°C. Total and Tyr1 phosphorylated Rpb1p were detected with the RNA pol II antibody and the RNA Pol II CTD phosphor Tyr1 antibody respectively (1:5000; Active Motif). Tdh1p were detected with anti-Tdh1p antibody (Thermofisher) and Rrp6p were detected using anti-Rrp6p antibody (Wasmuth and Lima, 2017). All secondary antibodies used were obtained from LI-COR (1:10000).

Co-immunoprecipitation—Samples were grown and harvested as previously stated. Cell lysates were prepared as indicated above, but with the Co-IP lysis buffer (50mM Tris-HCl pH 7.4, 50mM NaCl and 1% NP-40) supplemented with protease and phosphatase inhibitors (Roche). Approximately 1.5mg of protein lysates were incubated with 25uL of magnetic anti-HA beads (Pierce) for 1 h at 4°C. Samples were washed 6 times with lysis buffer and eluted in 40uL of 1 mg/mL HA Peptide (Sigma-Aldrich). 10uL of eluate and 5ug of total lysates were loaded onto each lane of a Nu-Page gel. Rrp6p was detected with anti-Rrp6 (1:5000, (Schuch et al., 2014)) and HA tagged proteins were detected with anti-HA (1:5000, ABM). Secondary antibodies used were obtained from LI-COR (1:10000).

QUANTIFICATION AND STATISTICAL ANALYSIS

RNA-Sequencing and data analysis—RNA-sequencing of samples was performed using biological triplicates. HISAT2 (version 2.1.0) (Kim et al., 2019) was used to align the reads to the *S. cerevisiae* reference genome (assembly 64–1-1) downloaded from Ensembl (https://useast.ensembl.org/index.html). HTseq-count (Anders et al., 2015) (with the option -s reverse) was used with the *S. cerevisiae* genome annotation (release 97) to calculate read counts. EdgeR (version 3.26.5) (Robinson et al., 2010) was used to conduct differential gene expression analysis between the wild-type and the *mpk1Δ* mutant, the wild-type and *rrp6Δ* mutant, and the wild-type and *mpk1Δrrp6Δ* mutants. Differentially expressed genes were selected based on the log fold change absolute value greater than 1 and the FDR q-value threshold 0.05. GO analysis was performed using GO Term Finder (version 0.86) (Boyle et al., 2004).

Supplementary Material

Refer to Web version on PubMed Central for supplementary material.

ACKNOWLEDGMENTS

We thank David E. Levin and Christopher D. Lima for their generous gift of the Mpk1 mutant plasmids and the α-RRP6 antibodies, respectively; Indya Weathers for her dedication and extensive technical assistance; and Yerbol Kurmangaliyev for his assistance in demultiplexing our RNA-seq data. This work was supported by the National Institute of General Medical Sciences grant R35 GM130370. C.W. and S.M.D. were supported by the National Research Service Award training grant GM007185.

REFERENCES

Allmang C, Kufel J, Chanfreau G, Mitchell P, Petfalski E, and Tollervey D (1999). Functions of the exosome in rRNA, snoRNA and snRNA synthesis. EMBO J. 18, 5399–5410. [PubMed: 10508172]

Anders S, Pyl PT, and Huber W (2015). HTSeq—a Python framework to work with high-throughput sequencing data. Bioinformatics 37, 166–169.

Andrulis ED, Werner J, Nazarian A, Erdjument-Bromage H, Tempst P, and Lis JT (2002). The RNA processing exosome is linked to elongating RNA polymerase II in Drosophila. Nature 420, 837–841. [PubMed: 12490954]

Babour A, Shen Q, Dos-Santos J, Murray S, Gay A, Challal D, Fasken M, Palancade B, Corbett A, Libri D, et al. (2016). The Chromatin Remodeler ISW1 Is a Quality Control Factor that Surveys Nuclear mRNP Biogenesis. Cell 167, 1201–1214.e15. [PubMed: 27863241]

Bernstein J, and Toth EA (2012). Yeast nuclear RNA processing. World J. Biol. Chem. 3, 7–26. [PubMed: 22312453]

Boyle EI, Weng S, Gollub J, Jin H, Botstein D, Cherry JM, and Sherlock G (2004). GO:TermFinder—open source software for accessing Gene Ontology information and finding significantly enriched Gene Ontology terms associated with a list of genes. Bioinformatics 20, 3710–3715. [PubMed: 15297299]

Brachmann CB, Davies A, Cost GJ, Caputo E, Li J, Hieter P, and Boeke JD (1998). Designer deletion strains derived from Saccharomyces cerevisiae S288C: a useful set of strains and plasmids for PCR-mediated gene disruption and other applications. Yeast 14, 115–132. [PubMed: 9483801]

Bresson S, Tuck A, Staneva D, and Tollervey D (2017). Nuclear RNA Decay Pathways Aid Rapid Remodeling of Gene Expression in Yeast. Mol. Cell 65, 787–800.e5. [PubMed: 28190770]

Burkard KT, and Butler JS (2000). A nuclear 3'-5' exonuclease involved in mRNA degradation interacts with Poly(A) polymerase and the hnRNA protein Npl3p. Mol. Cell. Biol. 20, 604–616. [PubMed: 10611239]

Butler JS, and Mitchell P (2010). Rrp6, Rrp47 and cofactors of the nuclear exosome. Adv. Exp. Med. Biol. 702, 91–104. [PubMed: 21618877]

Callahan KP, and Butler JS (2008). Evidence for core exosome independent function of the nuclear exoribonuclease Rrp6p. Nucleic Acids Res. 36, 6645–6655. [PubMed: 18940861]

Carmody SR, Tran EJ, Apponi LH, Corbett AH, and Wente SR (2010). The mitogen-activated protein kinase Slt2 regulates nuclear retention of non-heat shock mRNAs during heat shock-induced stress. Mol. Cell. Biol. 30, 5168–5179. [PubMed: 20823268]

de Nobel H, Ruiz C, Martin H, Morris W, Brul S, Molina M, and Klis FM (2000). Cell wall perturbation in yeast results in dual phosphorylation of the Slt2/Mpk1 MAP kinase and in an Slt2-mediated increase in FKS2-lacZ expression, glucanase resistance and thermotolerance. Microbiology 146, 2121–2132. [PubMed: 10974100]

Fasken MB, Losh JS, Leung SW, Brutus S, Avin B, Vaught JC, Potter-Birriel J, Craig T, Conn GL, Mills-Lujan K, et al. (2017). Insight into the RNA Exosome Complex Through Modeling Pontocerebellar Hypoplasia Type 1b Disease Mutations in Yeast. Genetics 205, 221–237. [PubMed: 27777260]

Feigenbutz M, Jones R, Besong TMD, Harding SE, and Mitchell P (2013a). Assembly of the yeast exoribonuclease Rrp6 with its associated cofactor Rrp47 occurs in the nucleus and is critical for the controlled expression of Rrp47. J. Biol. Chem. 288, 15959–15970. [PubMed: 23580640]

Feigenbutz M, Garland W, Turner M, and Mitchell P (2013b). The exosome cofactor Rrp47 is critical for the stability and normal expression of its associated exoribonuclease Rrp6 in Saccharomyces cerevisiae. PLoS ONE 8, e80752. [PubMed: 24224060]

Fox MJ, and Mosley AL (2016). Rrp6: Integrated roles in nuclear RNA metabolism and transcription termination. Wiley Interdiscip. Rev. RNA 7, 91–104. [PubMed: 26612606]

Fox MJ, Gao H, Smith-Kinnaman WR, Liu Y, and Mosley AL (2015). The exosome component Rrp6 is required for RNA polymerase II termination at specific targets of the Nrd1-Nab3 pathway. PLoS Genet 11, e1004999. [PubMed: 25680078]

Ghaemmaghami S, Huh WK, Bower K, Howson RW, Belle A, Dephe N, O'Shea EK, and Weissman JS (2003). Global analysis of protein expression in yeast. Nature 425, 737–741. [PubMed: 14562106]

Gietz RD, and Schiestl RH (2007). High-efficiency yeast transformation using the LiAc/SS carrier DNA/PEG method. Nat. Protoc. 2, 31–34. [PubMed: 17401334]

Gillespie A, Gabunilas J, Jen JC, and Chanfreau GF (2017). Mutations of EXOSC3/Rrp40p associated with neurological diseases impact ribosomal RNA processing functions of the exosome in *S. cerevisiae*. RNA 23, 466–472. [PubMed: 28053271]

Graham AC, Kiss DL, and Andrulis ED (2009). Core exosome-independent roles for Rrp6 in cell cycle progression. Mol. Biol. Cell 20, 2242–2253. [PubMed: 19225159]

Gustin MC, Albertyn J, Alexander M, and Davenport K (1998). MAP kinase pathways in the yeast Saccharomyces cerevisiae. Microbiol. Mol. Biol. Rev. 62, 1264–1300. [PubMed: 9841672]

Hahn J-S, and Thiele DJ (2002). Regulation of the Saccharomyces cerevisiae Slt2 kinase pathway by the stress-inducible Sdp1 dual specificity phosphatase. J. Biol. Chem. 277, 21278–21284. [PubMed: 11923319]

Jin C, Strich R, and Cooper KF (2014). Slt2p phosphorylation induces cyclin C nuclear-to-cytoplasmic translocation in response to oxidative stress. Mol. Biol. Cell 25, 1396–1407. [PubMed: 24554767]

Kanehisa M, and Goto S (2000). KEGG: kyoto encyclopedia of genes and genomes - Release 72.1, 12 1, 2014 Nucleic Acids Res. 28, 27–30. [PubMed: 10592173]

Kim K-Y, and Levin DE (2011). Mpk1 MAPK association with the Paf1 complex blocks Sen1-mediated premature transcription termination. Cell 144, 745–756. [PubMed: 21376235]

Kim K-Y, Truman AW, Caesar S, Schlenstedt G, and Levin DE (2010). Yeast Mpk1 cell wall integrity mitogen-activated protein kinase regulates nucleocytoplasmic shuttling of the Swi6 transcriptional regulator. Mol. Biol. Cell 21, 1609–1619. [PubMed: 20219973]

Kim D, Paggi JM, Park C, Bennett C, and Salzberg SL (2019). Graphbased genome alignment and genotyping with HISAT2 and HISAT-genotype. Nat. Biotechnol. 37, 907–915. [PubMed: 31375807]

Levin DE (2005). Cell wall integrity signaling in Saccharomyces cerevisiae. Microbiol. Mol. Biol. Rev. 69, 262–291. [PubMed: 15944456]

Longtine MS, McKenzie A 3rd, Demarini DJ, Shah NG, Wach A, Brachat A, Philippsen P, and Pringle JR (1998). Additional modules for versatile and economical PCR-based gene deletion and modification in Saccharomyces cerevisiae. Yeast 14, 953–961. [PubMed: 9717241]

Moraes KCM (2010). RNA surveillance: molecular approaches in transcript quality control and their implications in clinical diseases. Mol. Med. 16, 53–68. [PubMed: 19829759]

Morton DJ, Kuiper EG, Jones SK, Leung SW, Corbett AH, and Fasken MB (2018). The RNA exosome and RNA exosome-linked disease. RNA 24, 127–142. [PubMed: 29093021]

Parent SA, Fenimore CM, and Bostian KA (1985). Vector systems for the expression, analysis and cloning of DNA sequences in S. cerevisiae. Yeast 1, 83–138. [PubMed: 3916863]

Parker R (2012). RNA degradation in Saccharomyces cerevisae. Genetics 191, 671–702. [PubMed: 22785621]

Robinson MD, McCarthy DJ, and Smyth GK (2010). edgeR: a Bioconductor package for differential expression analysis of digital gene expression data. Bioinformatics 26, 139–140. [PubMed: 19910308]

Roy K, and Chanfreau G (2014). Stress-induced nuclear RNA degradation pathways regulate yeast bromodomain factor 2 to promote cell survival. PLoS Genet 10, e1004661. [PubMed: 25232960]

Russo P, Kalkkinen N, Sareneva H, Paakkola J, and Makarow M (1992). A heat shock gene from Saccharomyces cerevisiae encoding a secretory glycoprotein. Proc. Natl. Acad. Sci. USA 89, 3671–3675. [PubMed: 1570286]

Schuch B, Feigenbutz M, Makino DL, Falk S, Basquin C, Mitchell P, and Conti E (2014). The exosome-binding factors Rrp6 and Rrp47 form a composite surface for recruiting the Mtr4 helicase. EM BO J. 33, 2829–2846.

Sloan KE, Schneider C, and Watkins NJ (2012). Comparison of the yeast and human nuclear exosome complexes. Biochem. Soc. Trans. 40, 850–855. [PubMed: 22817747]

Van Oss SB, Cucinotta CE, and Arndt KM (2017). Emerging Insights into the Roles of the Paf1 Complex in Gene Regulation. Trends Biochem. Sci. 42, 788–798. [PubMed: 28870425]

Volanakis A, Passoni M, Hector RD, Shah S, Kilchert C, Granneman S, and Vasiljeva L (2013). Spliceosome-mediated decay (SMD) regulates expression of nonintronic genes in budding yeast. Genes Dev. 27, 2025–2038. [PubMed: 24065768]

Wan J, Yourshaw M, Mamsa H, Rudnik-Schöneborn S, Menezes MP, Hong JE, Leong DW, Senderek J, Salman MS, Chitayat D, et al. (2012). Mutations in the RNA exosome component gene EXOSC3 cause pontocerebellarhypoplasia and spinal motor neuron degeneration. Nat. Genet. 44, 704–708. [PubMed: 22544365]

Wasmuth EV, and Lima CD (2017). The Rrp6 C-terminal domain binds RNA and activates the nuclear RNA exosome. Nucleic Acids Res. 45, 846–860. [PubMed: 27899565]

Winzeler EA, Shoemaker DD, Astromoff A, Liang H, Anderson K, Andre B, Bangham R, Benito R, Boeke JD, Bussey H, et al. (1999). Functional characterization of the S. cerevisiae genome by gene deletion and parallel analysis. Science 285, 901–906. [PubMed: 10436161]

Yurko N, Liu X, Yamazaki T, Hoque M, Tian B, and Manley JL (2017). MPK1/SLT2 Links Multiple Stress Responses with Gene Expression in Budding Yeast by Phosphorylating Tyr1 of the RNAP II CTD. Mol. Cell 68, 913–925.e3. [PubMed: 29220656]

Zinder JC, and Lima CD (2017). Targeting RNA for processing or destruction by the eukaryotic RNA exosome and its cofactors. Genes Dev. 31, 88–100. [PubMed: 28202538]

Highlights

- Rrp6 exhibits negative genetic interactions with the elongation factors Mpk1 and Paf1
- Rrp6 functions during stress independently from the RNA exosome
- Mpk1 and Rrp6 mutants share many downregulated genes during heat stress
- Overexpression of *HSP150* rescues lethality of the *mpk1Δrrp6Δ* mutant during stress

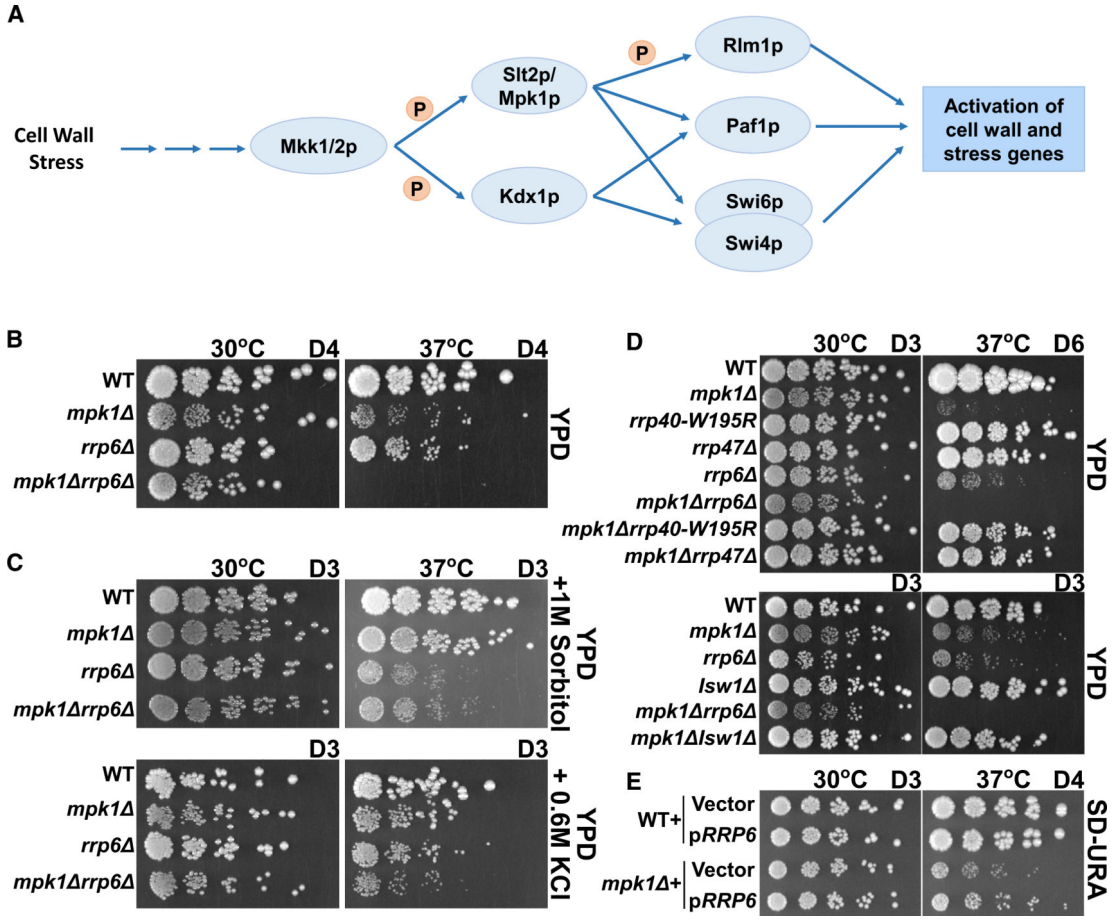

Figure 1. Genetic Interaction between Mpk1p, Rrp6p, and Nuclear RNA Exosome or Rrp6-Associated Proteins

(A) The cell wall integrity (CWI) pathway, according to the model proposed by Kanehisa and Goto (2000).

(B) Genetic interactions between Mpk1p and Rrp6p. WT strain is derived from BY4742 (Brachmann et al., 1998) and single knockout strains were obtained from (Winzeler et al., 1999).

(C) The negative genetic interaction between the *mpk1Δ* and *rrp6Δ* mutants can be rescued by osmotic support.

(D) Deletion or mutation of Rrp6-associated proteins (Rrp40p, Rrp47p, and Isw1p) rescues the heat sensitivity of the *mpk1Δ* mutant.

(E) Overexpression of Rrp6p partially rescues the heat sensitivity of the *mpk1Δ* mutant.

For panels (B)—(E), 5-fold serial dilutions of indicated strains were spotted onto the respective plates. Plates were grown at 30°C, 35°C, or 37°C for the indicated number of days.

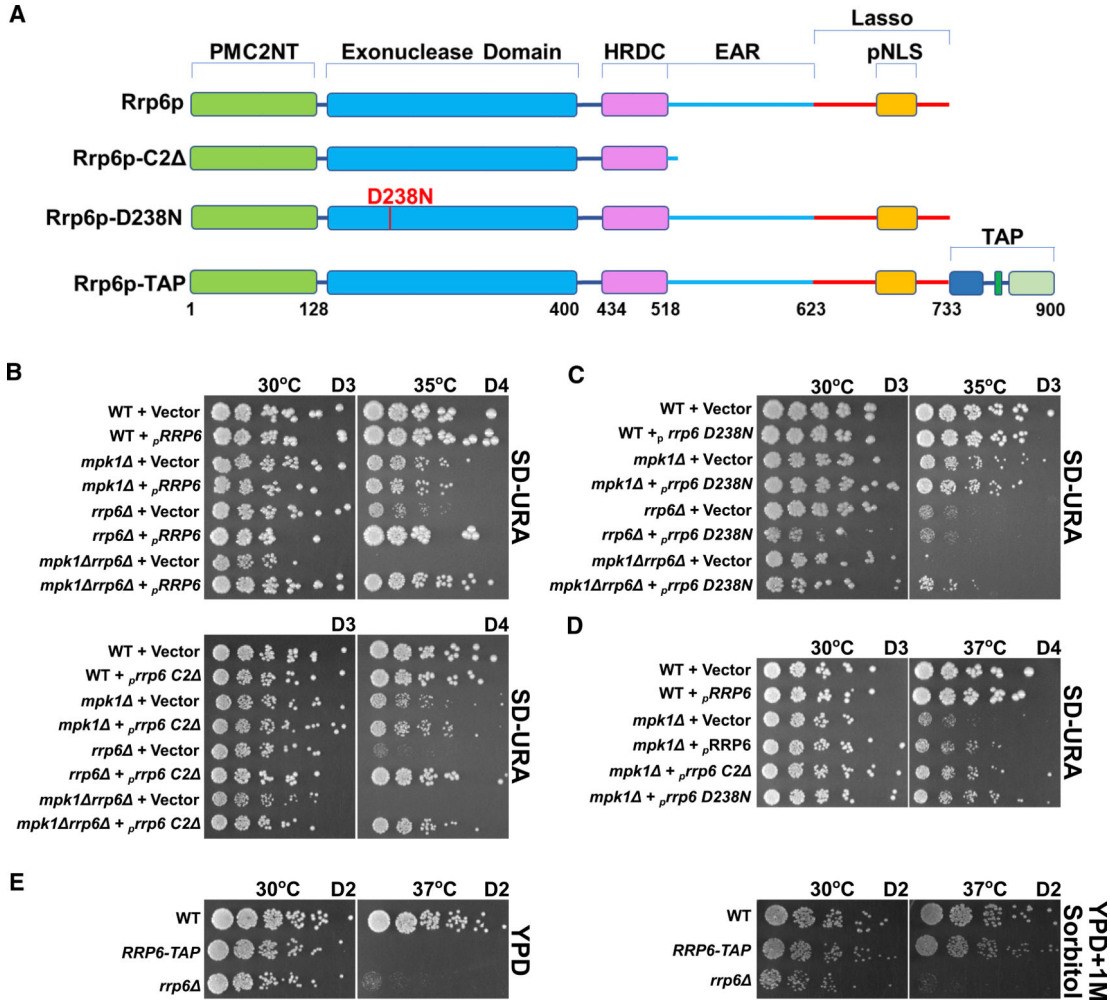

Figure 2. Contribution of Rrp6p Structural Domains to Cell Survival in Stress Conditions

(A) Schematic diagram of Rrp6p and its various mutants. Domain structure of Rrp6p is shown according to Wasmuth and Lima (2017). The TAP tag consists of a calmodulin-binding peptide followed by a TEV protease cleavage site and two protein A domains.

(B) Serial dilution growth analysis of strains expressing WT or *C2Δ* versions of Rrp6p.

(C) Serial dilution growth analysis of strains expressing the WT *RRP6* or *D238N* mutant version of Rrp6p.

(D) Overexpression of Rrp6p or of its mutants can suppress the ts defect of the *mpk1Δ* mutant.

(E) Serial diluation growth analysis of WT, *RRP6-TAP* (Ghaemmaghami et al., 2003), and *rrp6Δ* strains. For all panels,yeast cultures were spotted onto the indicated media plates and grown for the indicated number of days at the indicated temperatures.

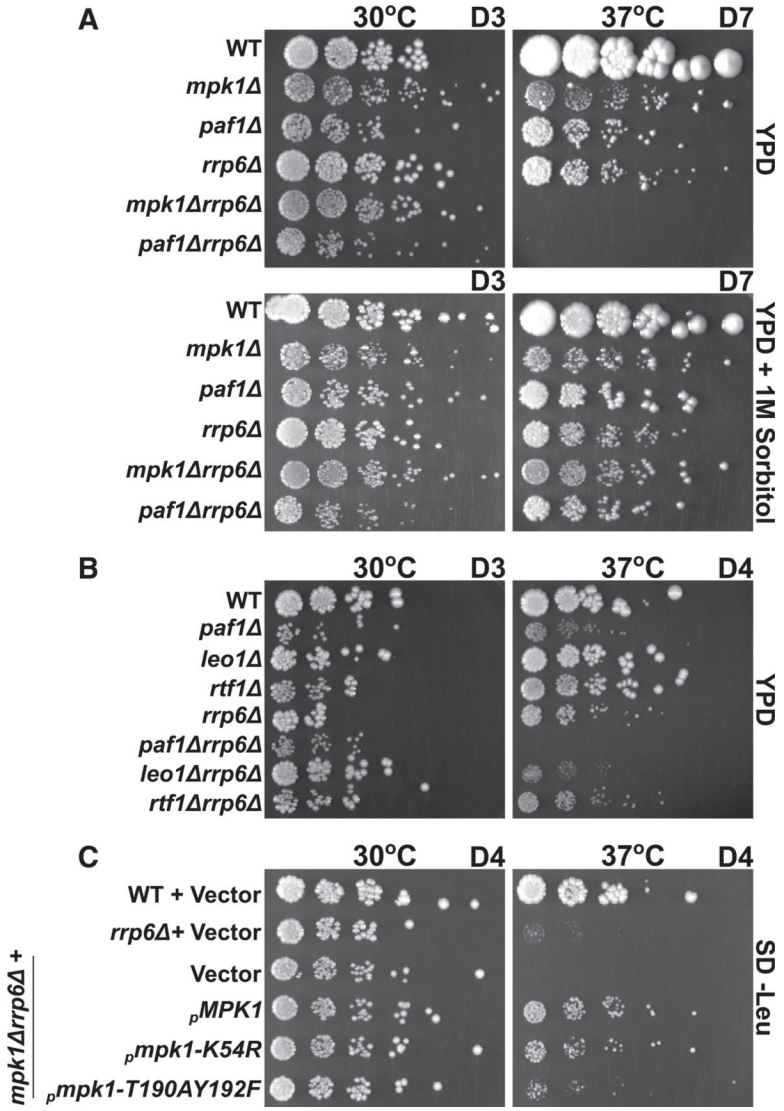

Figure 3. Rrp6p Function in the Heat Stress Response Pathway Requires Paf1p and Its Interaction with an Activated Mpk1p

(A) Genetic interactions between *mpk1Δ*, *paf1Δ*, and *rrp6Δ*.

(B) Genetic interactions between *rrp6Δ* and Paf1c complex mutants.

(C) Synthetic lethality of the *mpk1Δrrp6Δ* mutant at high temperature can be rescued by a catalytically inactive Mpk1p. For all panels, 5-fold serial dilution of liquid cultures of the indicated strains were grown at the indicated temperatures and growth media for the indicated number of days.

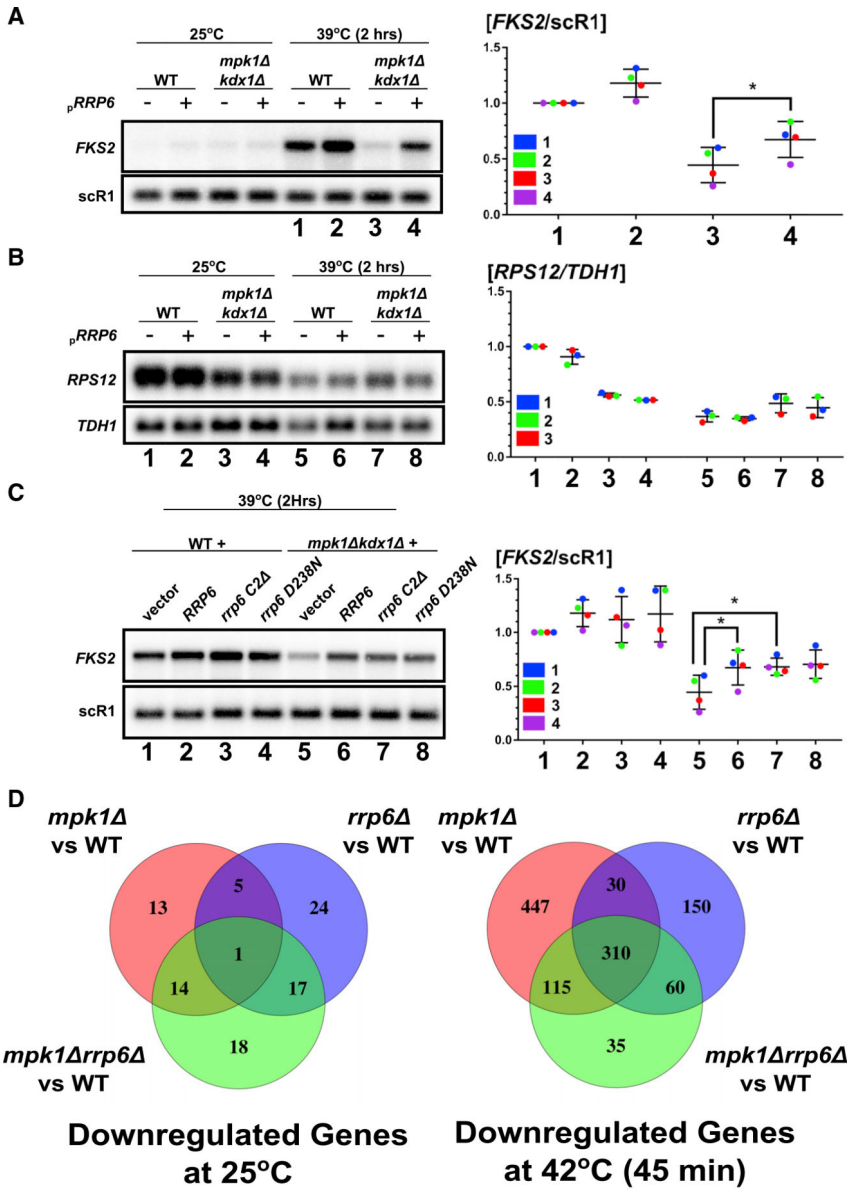

Figure 4. Rrp6p Is Required for Proper Expression of CWI Genes along with Mpk1p

(A) Representative northern blot analysis and quantification of *FKS2* levels in WT and *mpk1Δkdx1Δ* strains with or without Rrp6 overexpression. scR1 was used as a loading control.

(B) Representative northern blot analysis and quantification of *RPS12* levels in WT and *mpk1Δkdx1Δ* strains with or without Rrp6 overexpression. *TDH1* was used as a loading control.

(C) Expression of the *rrp6-C2Δ* mutant can rescue the *FKS2* expression defect of the *mpk1Δkdx1Δ* mutant. For panels (A—C), three to four biological replicates were performed with the relative levels of the gene of interest, and standard deviation is indicated on the right (*p < 0.033, paired t test).

(D) Venn diagram of genes down regulated in the *mpk1Δ*, *rrp6Δ*, and *mpk1Δrrp6Δ* mutants compared to WT before (25°C) and after a 45-min heat shock at 42°C.

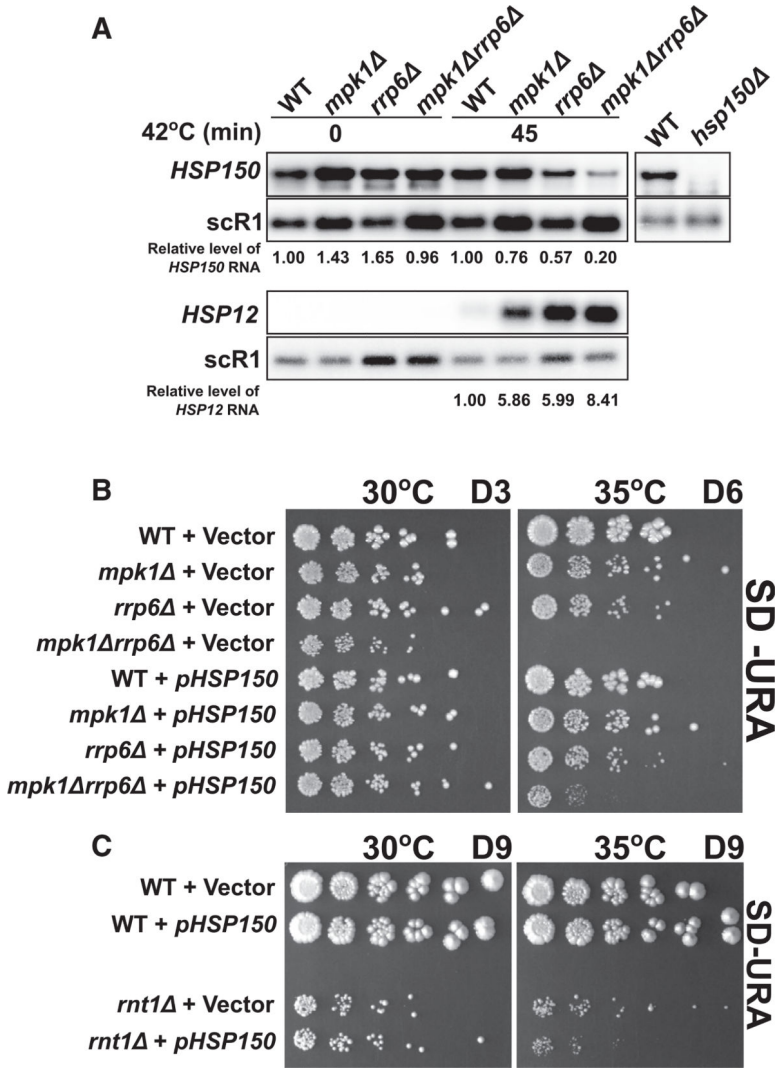

Figure 5. The Cell Wall Protein Hsp150p Is Not Expressed Properly in the *mpk1Δrrp6Δ* Mutant and Can Rescue the Heat Sensitivity of This Mutant

(A) Northern blot analysis of *HSP150* and *HSP12* expression in the indicated strains and conditions.

(B) Overexpression of *HSP150* can partially suppress the ts phenotype of the *mpk1Δrrp6Δ* mutant.5-fold serial dilution of the indicated strains were incubated on SD-URA plates at 30°C or 35°C for the indicated number of days.

(C) Overexpression of *HSP150* does not suppress the ts phenotype of the *rnt1Δ* mutant. Experimental details as in (B).

KEY RESOURCES TABLE

REAGENT or RESOURCE	SOURCE	IDENTIFIER
Antibodies		
Mouse anti-HA (clone HA.C5)	ABM	Cat #G036; RRID: AB_2616604
Rabbit anti-Rrp6	(Wasmuth and Lima, 2017)	N/A
IRDye® 680RD Goat anti-Rabbit	LI-COR	Cat #926–68071; RRID: AB_10956166
IRDye® 800CW Goat anti-Mouse	LI-COR	Cat #926–32210; RRID: AB_621842
IRDye® 680RD Goat anti-Rat	LI-COR	Cat #926–68076; RRID: AB_10956590
TDH1 Monoclonal Antibody	Thermofisher Scientific	Cat #MA5–15738; RRID: AB_10977387
RNA Pol II CTD phospho Tyr1 antibody (clone 3D12)	Active Motif	Cat #61384; RRID: AB_2793613
RNA pol II antibody (clone 4H8)	Active Motif	Cat #39497; RRID: AB_2732926
Chemicals, Peptides, and Recombinant Proteins		
Phenol: chloroform: iso-amyl alcohol (25:24:1)	Miiiipore Sigma	Cat #6810
OuikChange Lightning Site-Directed Mutagenesis Kit	Agilent	Cat #210518
Fast-Fusion Cloning kit	Tonkbio	Cat # TB10012A
Pierce Anti-HA Magnetic Beads	Thermofisher Scientific	Cat #88836
Influenza Hemagglutinin (HA) Peptide	Sigma-Aldrich	Cat# 12149
T3 RNA polymerase	Promega	Cat #P2083
T4 polynucleotide kinase	New England BioLabs	Cat# M0201S
α-^{32}P-UTP	Perkin Elmer	Cat #BLU507Z001 MC
γ-^{32}P-ATP	Perkin Elmer	Cat #BLU502A500UC
NuPAGE 4–12% Bis-Tris Protein Gels	Thermofisher Scientific	Cat # NP0321 BOX
Critical Commercial Assays		
TruSeq Stranded RNA HT Kit	Illumina	Cat#15032620
Deposited Data		
RNA-Seq of heat shocked samples	This paper	GEO: GSE140504
Experimental Models: Organisms/Strains		
S. cerevisiae strains (See Table S2)	This paper	N/A
Oligonucleotides		
Plasmid construction and mutagenesis (See Table S4)	This paper	N/A
Probe sequence for scR1: ATCCCGGCCGCCTCCATCAC	This paper	N/A
Probe sequence for ITS2: AGGCCAGCAATTTCAAGTTAACTCC	This paper	N/A
HSP150 T3 Riboprobe (See Table S3)	This paper	N/A
3xHA Tagging of Mpk1 p (See Table S3)	This paper	N/A
Recombinant DNA		
Plasmids transformed in *S. cerevisiae* (See Table S3)	This paper	N/A
Software and Algorithms		
HISAT2	(Kirnet al. 2019)	RRID:SCR_015530
HTseq-count	(Anders et ai,, 2015)	RRID:SCR_011867

REAGENT or RESOURCE	SOURCE	IDENTIFIER
edgeR	(Robinson et al., 2010)	RRID:SCR_012802
GO Term Finder	(Boyle et al., 2004)	RRID:SCR_008870